ISSN: 1813-4890

Study on nonlinear dynamic characteristics of two-rotor vibrating screen under material impact

Jie Leng [a], Yongjun Hou [b], Pan Fang [c], Chaoyang Xiang and Ruihao Peng

School of Mechanical Engineering, Southwest Petroleum University, Chengdu 610500, China;

[a]1441348358@qq.com, [b]yongjunhou@126.com, [c]ckfangpan@126.com

Abstract

The interaction between the material and the vibrating screen during the screening process was considered, and a study was conducted on the dual-rotor vibrating screen under material impact. The differential equation of motion of the system is established by using the generalized Lagrange equation, the steady-state amplitude response of the vibrating body is solved. Combined with the coupling effect of vibrating body and material, the impact equation and boundary conditions of the system are established, and the general solution of nonlinear disturbance and Poincaré mapping cross section of the system are obtained. The nonlinear dynamic characteristics of the system under material impact were described using numerical analysis. The results show that with the increase of the mass ratio of material to vibrating body, the motion of the system doubles from stable single-periodic motion to multi-periodic motion, finally evolves into chaotic motion. The study reveals the nonlinear dynamic characteristics of the dual-rotor vibrating system under material impact, providing guidance for the design optimization of vibrating screens.

Keywords

Material impact; Poincare mapping; Bifurcation; Stability of synchronization.

1. Introduction

During the screening process of materials, material impact may have an impact on the synchronization and stability of the vibration system [1]. Especially when the mass of the material is large, it is easy to cause sudden changes in the velocity of the vibrating body and the phase difference of the eccentric rotor. Therefore, an in-depth study of the coupling effect between the material and the vibration system, revealing the working principle of the system has important scientific significance and engineering value for optimizing the design of vibration machinery.

At present, some scholars have conducted researches based on the interaction between material and vibrating body. Kong et al. [2-3] analyzed the motion state of materials under different vibration conditions based on Coulomb friction law and collision principle, and used an improved multi-modal incremental harmonic balance method to comprehensively study the interaction between friction and material impact, revealing that the interaction between materials and vibrating feeders cannot be ignored. Wang et al. [4-5] used a discrete-finite element method (DEM-FEM) for data coupling to determine the response of the screen mesh under impact force, and obtained the stress and deformation distribution on the surface of the screen mesh under material action. They proposed effective methods to reduce the impact force and optimized the layout of the support beam. Huang et al. [6-7] combined cross-coupling control strategy with adaptive global sliding mode control algorithm to study the speed and phase synchronization control problem of the two eccentric rotors in the variable load torque nonlinear vibration system. They further applied the ACCC strategy and AGSMC algorithm

ISSN: 1813-4890

controller to the multi-exciter vibration system considering material effect and improved the control accuracy, achieving zero phase difference synchronization of adjacent exciters. Hou et al. [8-9] studied the stability of the dual-rotor vibration system considering material effect, analyzed the law of action of materials with different masses, and verified the vertical amplitude response of the vibration body through experiments. Although the impact of materials on the vibration system has been studied, considering the double eccentric rotors as a stable rotating motion or keeping them synchronized through control methods ignores the interactive effects of material impact. In addition, under the actual working conditions, the vibrating body will vibrate both vertically and horizontally. Only the vertical amplitude response of the vibrating body is limited, and the corresponding phase of the material at each moment under the impact force is not clearly explained.

The purpose of this study is to conduct a comprehensive analysis of the nonlinear dynamic behavior of a three degree of freedom vibration system. By studying the periodic collision behavior between materials and vibrating bodies, the impact of material impact on system synchronization and stability is revealed. Based on the nonlinear dynamics theory of vibration systems, this paper explores the motion laws of materials and vibrating screens during their interaction, providing a theoretical basis for the further development and design of vibrating screens

2. Dynamic model of vibration system

The dynamic model of dual-rotor vibration system under material impact is shown in Fig. 1(a). This system is composed of a box, vibration motor, supporting springs, and base, among others. The two eccentric rotors are respectively driven by a vibration motor with a set speed of ω_m(rad/s) and perform reverse rotation. The distance between the system centroid and the motor axis is l_i(m); The inclination angle of the motor is β(rad); The instantaneous phase angle and eccentricity of two eccentric rotors are φ_i(rad) and r_i(m); The inclination angle between the screen surface and the horizontal angle is δ(rad). The system motion includes horizontal vibration x and vertical vibration y, as well as oscillation around the center of mass ψ. The box body is connected to the base through a support spring and the mass of the box body is m_0(kg); The spring stiffness coefficient and damping coefficient are expressed as k_j and f_j, respectively (j=x, y, ψ). In addition, the material is considered as a mass block acting on the sieve, with a mass of m_w (kg).

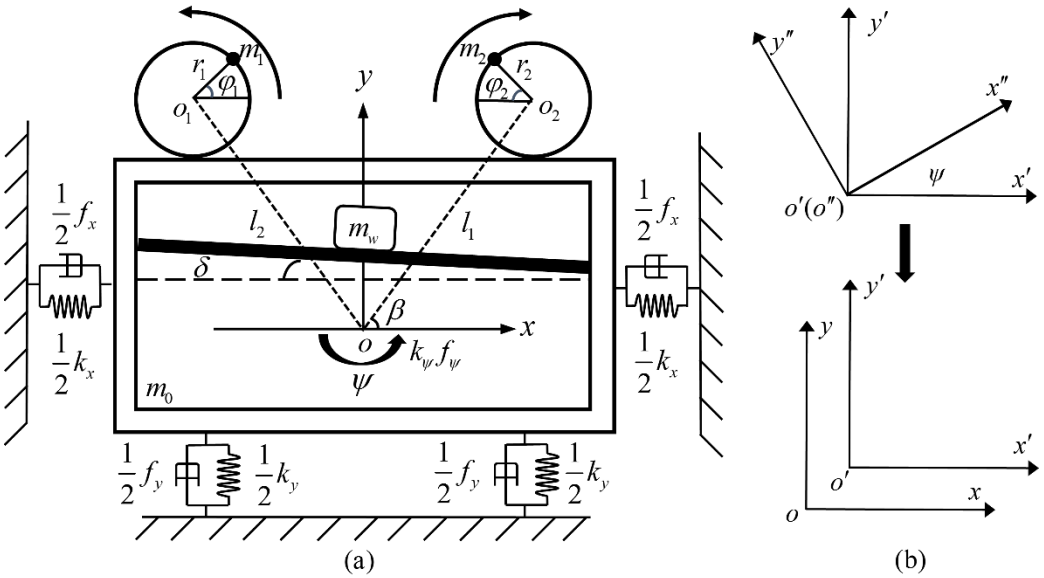

Fig. 1. (a) Dynamic model; (b) Coordinate transformation method

ISSN: 1813-4890

As shown in Fig. 1 (b), set three coordinate systems: fixed coordinate system, moving coordinate system, and rotating coordinate system. After converting from a rotating coordinate system to a fixed coordinate system, the eccentric rotor coordinates are represented as:

$$\Phi_1 = \begin{bmatrix} x + r_1\, cos(\varphi_1 + \psi) - l_1\, cos(\beta - \psi) \\ y + r_1\, sin(\varphi_1 + \psi) + l_1\, sin(\beta - \psi) \end{bmatrix};\ \Phi_2 = \begin{bmatrix} x - r_2\, cos(\varphi_2 - \psi) + l_2\, cos(\beta + \psi) \\ y + r_2\, sin(\varphi_2 - \psi) + l_2\, sin(\beta + \psi) \end{bmatrix} \quad (1)$$

Here, take q=[x, y, ψ, φ_1, φ_2]^T as the generalized coordinate matrix of the system, and Q=[0, 0, 0, M_{e1}-R_{e1}, M_{e2}-R_{e2}]^T as the generalized force matrix of the system. The kinetic energy T, potential energy V, and dissipative energy D at system stabilization are expressed as:

$$T = \frac{1}{2}m(\dot{x}^2 + \dot{y}^2) + \frac{1}{2}J_m\dot{\psi}^2 + \frac{1}{2}\sum_{i=1}^{2} J_{0i}\,\dot{\varphi_i}^2 + \frac{1}{2}\sum_{i=1}^{2} m_i\dot{\Phi_i}^T\,\dot{\Phi_i}$$

$$V = \frac{1}{2}k_x x^2 + \frac{1}{2}k_y y^2 + \frac{1}{2}k_\psi \psi^2, D = \frac{1}{2}f_x\dot{x}^2 + \frac{1}{2}f_y\dot{y}^2 + \frac{1}{2}f_\psi\dot{\psi}^2 + \frac{1}{2}f_1\dot{\varphi_1}^2 + \frac{1}{2}f_2\dot{\varphi_2}^2 \quad (2)$$

The generalized Lagrange equation is introduced to establish the differential equation of motion of the dynamics model:

$$\frac{d}{dt}\left(\frac{\partial T}{\partial \dot{q}_i}\right) - \frac{\partial T}{\partial q_i} + \frac{\partial V}{\partial q_i} + \frac{\partial D}{\partial \dot{q}_i} = Q \quad (3)$$

Take M=m_0+m_1+m_2+m_w as the total mass of the system, substituting kinetic energy T, potential energy V and dissipated energy D into Lagrange equation, the system dynamics equation can be obtained:

$$\begin{aligned}
&M\ddot{x} + f_x\dot{x} + k_x x = m_1 r_1(\dot{\varphi_1}^2\, cos\,\varphi_1 + \ddot{\varphi}_1\, sin\,\varphi_1) - m_2 r_2(\dot{\varphi_2}^2\, cos\,\varphi_2 + \ddot{\varphi}_2\, sin\,\varphi_2)\\
&M\ddot{y} + f_y\dot{y} + k_y y = m_1 r_1(\dot{\varphi_1}^2\, sin\,\varphi_1 - \ddot{\varphi}_1\, cos\,\varphi_1) + m_2 r_2(\dot{\varphi_2}^2\, sin\,\varphi_2 - \ddot{\varphi}_2\, cos\,\varphi_2)\\
&J\ddot{\psi} + f_\psi\dot{\psi} + k_\psi\psi = -m_1 r_1 l_1[\dot{\varphi_1}^2\, sin(\beta + \varphi_1) - \ddot{\varphi}_1\, cos(\beta + \varphi_1)]\\
&\qquad + m_2 r_2 l_2[\dot{\varphi_2}^2\, sin(\beta + \varphi_2) - \ddot{\varphi}_2\, cos(\beta + \varphi_2)]\\
&J_{01}\ddot{\varphi}_1 + f_1\dot{\varphi}_1 = T_{e1} - m_1 r_1(\ddot{y}\, cos\,\varphi_1 - \ddot{x}\, sin\,\varphi_1 - l_1\ddot{\psi}\, cos(\varphi_1 + \beta) - l_1\dot{\psi}^2\, sin(\varphi_1 + \beta))\\
&J_{02}\ddot{\varphi}_2 + f_2\dot{\varphi}_2 = T_{e2} - m_2 r_2(\ddot{y}\, cos\,\varphi_2 + \ddot{x}\, sin\,\varphi_2 + l_2\ddot{\psi}\, cos(\varphi_2 + \beta) + l_2\dot{\psi}^2\, sin(\varphi_2 + \beta)) \quad (4)
\end{aligned}$$

Where, $\dot{\Delta} = d\Delta/\mathrm{d}t$, $\ddot{\Delta} = d^2\Delta/\mathrm{d}t^2$; J_{0i} represents the moment of inertia of excitation motor i; J represents the total moment of inertia of the system, which can be approximated as $J \approx Ml_e^2$, l_e is the equivalent radius around which the vibrating body revolves; f_i denotes the damping coefficient of the excitation motor, and T_{ei} represents the electromagnetic output torque of motor i.

To simplify the solution process, the following parameters are introduced:

$$\omega_x = \sqrt{\frac{k_x}{M}}, \xi_x = \frac{f_x}{2\sqrt{k_x M}}, n_x = \frac{\omega_x}{\omega_m}, \omega_y = \sqrt{\frac{k_y}{M}}, \xi_y = \frac{f_y}{2\sqrt{k_y M}}, n_y = \frac{\omega_y}{\omega_m}$$

$$\omega_\psi = \sqrt{k_\psi/J_m}, \xi_\psi = f_\psi/(2\sqrt{k_\psi J_m}), n_\psi = \omega_\psi/\omega_m, \eta_1 = m_1/M, \eta_2 = m_2/M, r_l = l/l_e, l_e = \sqrt{J/M}$$

$$\eta_j = \xi_j\omega_j, \omega_{dj} = \omega_j\sqrt{1 - \xi_j^2}, \gamma_j = arctan(2\xi_j n_j/1 - n_j^2),\ \rho_j = 1/\sqrt{(1 - n_j^2)^2 + (2\xi_j n_j)^2} \quad (5)$$

By using modal superposition method, the steady-state responses of the system in all directions are obtained as follows:

$$\begin{aligned}
x &= e^{-\eta_x t}(a_x\, sin\,\omega_{dx}\, t + b_x\, cos\,\omega_{dx}\, t) + r\rho_x[\eta_1\, cos(\varphi_1 - \gamma_x) - \eta_2\, cos(\varphi_2 - \gamma_x)]\\
y &= e^{-\eta_y t}(a_y\, sin\,\omega_{dy}\, t + b_y\, cos\,\omega_{dy}\, t) + r\rho_y[\eta_1\, sin(\varphi_1 - \gamma_y) + \eta_2\, sin(\varphi_2 - \gamma_y)]
\end{aligned}$$

ISSN: 1813-4890

$$\psi = e^{-\eta_\psi t}(a_\psi \sin\omega_{d\psi} t + b_\psi \cos\omega_{d\psi} t) - \frac{rr_l}{l}\rho_\psi[\eta_1 \sin(\varphi_1 + \beta - \gamma_\psi) + \eta_2\rho_\psi \sin(\varphi_2 + \beta - \gamma_\psi)] \quad (6)$$

Where, the constants a_j and b_j are integration constants determined by the initial conditions and modal parameters of the system.

During the screening process, materials mainly perform throwing motion. The screening state of materials can be divided into two stages: contact stage and non-contact stage. When the material does not contact the sieve surface, small factors such as air friction are ignored, and the material is only subjected to gravity. Therefore, the differential equation of the movement of the material in the non-collision phase can be expressed as:

$$\ddot{y}_{m_w} = g; \dot{y}_{m_w} = gt + c_1; y_{m_w} = gt^2/2 + c_1 t + c_2 \quad (7)$$
$$\ddot{y}_{m_w} = g; \dot{y}_{m_w} = gt + c_1; y_{m_w} = gt^2/2 + c_1 t + c_2$$

Where, c_1 and c_2 are constants that depend on the initial conditions.

Introducing the coefficient of restitution into the law of conservation of momentum, the impact equation between the vibrating body M and the material m_w are obtained as:

$$\mu_m\dot{x}_{M+} + \dot{x}_{m_w+} = \mu_m\dot{x}_{M-} + \dot{x}_{m_w-}, \dot{x}_{M+} - \dot{x}_{M-} = R(\dot{x}_{m_w-} - \dot{x}_{M-})$$
$$\mu_m\dot{y}_{M+} + \dot{y}_{m_w+} = \mu_m\dot{y}_{M-} + \dot{y}_{m_w-}, \dot{y}_{M+} - \dot{y}_{M-} = R(\dot{y}_{m_w-} - \dot{y}_{M-}) \quad (8)$$

where, μ_m=M/m_w; R is the coefficient of restitution; $\dot{x}_{M-}$, $\dot{x}_{M+}$ and $\dot{y}_{M-}$, $\dot{y}_{M+}$ represent the instantaneous velocities of the vibrating body M along the x and y directions before and after collision, respectively; $\dot{x}_{m_w-}$, $\dot{x}_{m_w+}$ and $\dot{y}_{m_w-}$, $\dot{y}_{m_w+}$ represent the instantaneous velocities of the material along the x and y directions before and after collision, respectively.

Assuming that at the instant when the vibrating body M collides with the material m_w, the non-dimensional time t is 0, and at the instant before the next mutual collision, the non-dimensional time t is $2n\pi/\omega_m$. The boundary conditions for the displacement of the system under impact are obtained as follows:

$$x_M(0) = x_M(2n\pi/\omega_m) = x_{m_w}(0) = x_{m_w}(2n\pi/\omega_m) = x_{M0}$$
$$y_M(0) = y_M(2n\pi/\omega_m) = y_{m_w}(0) == y_{m_w}(2n\pi/\omega_m) = y_{M0} \quad (9)$$

Where, x_{M0} and y_{M0} represent the initial displacement of the vibrator that is the same as that of the material. $x_M(T)$, $x_{m_w}(T)$ and $y_M(T)$, $y_{m_w}(T)$ represent the displacements of the vibrator and material along the x and y directions at time T (T=0, $2n\pi/\omega_m$).

Furthermore, the boundary conditions for velocity are obtained as:

$$\dot{x}_M(0) = \frac{1-\mu R}{1+\mu}\dot{x}_M(2n\pi/\omega_m) + \frac{\mu(1+R)}{1+\mu}\dot{x}_{m_w}(2n\pi/\omega_m) = \dot{x}_{M0}$$
$$\dot{y}_M(0) = \frac{1-\mu R}{1+\mu}\dot{y}_M(2n\pi/\omega_m) + \frac{\mu(1+R)}{1+\mu}\dot{y}_{m_w}(2n\pi/\omega_m) = \dot{y}_{M0}$$
$$\dot{x}_{m_w}(0) = \frac{1+R}{1+\mu}\dot{x}_M(2n\pi/\omega_m) + \frac{\mu-R}{1+\mu}\dot{x}_{m_w}(2n\pi/\omega_m) = \dot{x}_{m_w0}$$
$$\dot{y}_{m_w}(0) = \frac{1+R}{1+\mu}\dot{y}_M(2n\pi/\omega_m) + \frac{\mu-R}{1+\mu}\dot{y}_{m_w}(2n\pi/\omega_m) = \dot{y}_{m_w0} \quad (10)$$

Where, $\dot{x}_{M0}$, $\dot{y}_{M0}$ and $\dot{x}_{m_w0}$, $\dot{y}_{m_w0}$ represent the initial velocities of the vibrating body and material; $\dot{x}_M(T)$, $\dot{x}_{m_w}(T)$ and $\dot{y}_M(T)$, $\dot{y}_{m_w}(T)$ represent the velocities of the vibrating body and material along the x and y directions at time T.

3. Nonlinear numerical analysis of vibration systems

In order to further explore the relationship between system stability and parameter variation, numerical simulation is used to analyze the influence of different quality materials on the

ISSN: 1813-4890

nonlinear dynamic characteristics of the system. Assuming that the two drive motors have the same parameters, the basic parameters of the system are set as follows:

Table 1 Essential parameters of the system

Vibrating body	Eccentric rotors	Electrical parameters	Motor parameters
m_0=100 (kg)	m_1=4 (kg)	P_e=0.12 (kw)	n_p=2
k_x=89586 (N/m)	m_2=6 (kg)	V=380 (V)	ω_m=157 (rad/s)
k_y=89586 (N/m)	r=0.03 (m)	I= 0.4(A)	R_s=0.435(Ω)
k_ψ=13560 (N·m/rad)	l=0.30 (m)	f_0=50 (Hz)	R_r=0.816(Ω)
f_x=239 (N·s/m)	β=60°	/	L_s=0.001(H)
f_y=139 (N·s/m)	/	/	L_r=0.002(H)
f_ψ=30 (N·m·s /rad)	/	/	L_m=0.0069(H)
J_m=8 (kg·m^2)	/	/	/

3.1. System dynamics characteristics of different material masses

Fig. 2 shows the dynamic characteristics of the vibration system under the impact of 1kg material. In the screening process, the displacement response of the vibrating body along the x, y and ψ directions is shown in Fig. 2(a), (b) and (c). Compared with the operation without load, the amplitude of the vibrator impacted by the material fluctuates significantly in all directions. When the system runs stably, the phase diagram tracks in the x, y and ψ directions overlap with an ellipse, indicating that the vibrating body moves in a stable single period in all directions, as shown in Fig. 2(d), (e) and (f). The trajectory of the center of mass of the vibrating screen tends to be elliptical, as shown in Fig. 2(g). In the screening process, the motor speed was stable at 157rad/s and was not affected by the impact of the material, as shown in Fig. 2(h). When m_w=1kg, compared with no material (m_w=0kg), the rotor stability phase difference of the two motors increases to 0.052rad. The instantaneous phase difference changes slightly when the material collides with the screen, and the mutation values are all 0.012rad, but the synchronous phase difference gradually becomes stable under the system's self-synchronous coupling, as shown in Fig. 2(i). In summary, the phase difference between the two motors presents an approximate periodic micro-mutation under the action of materials, indicating that the internal coupling synchronization relationship of the system ensures that the system dynamics characteristics are not significantly unstable under the impact of materials with a mass of 1kg.

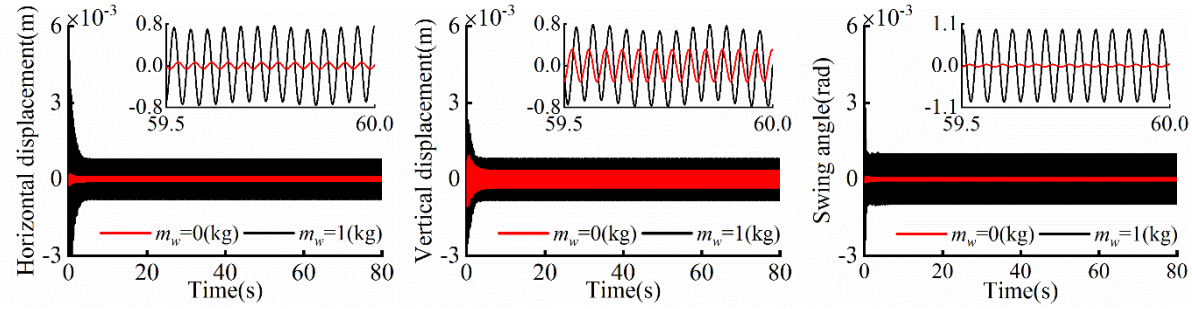

(a) (b) (c)

ISSN: 1813-4890

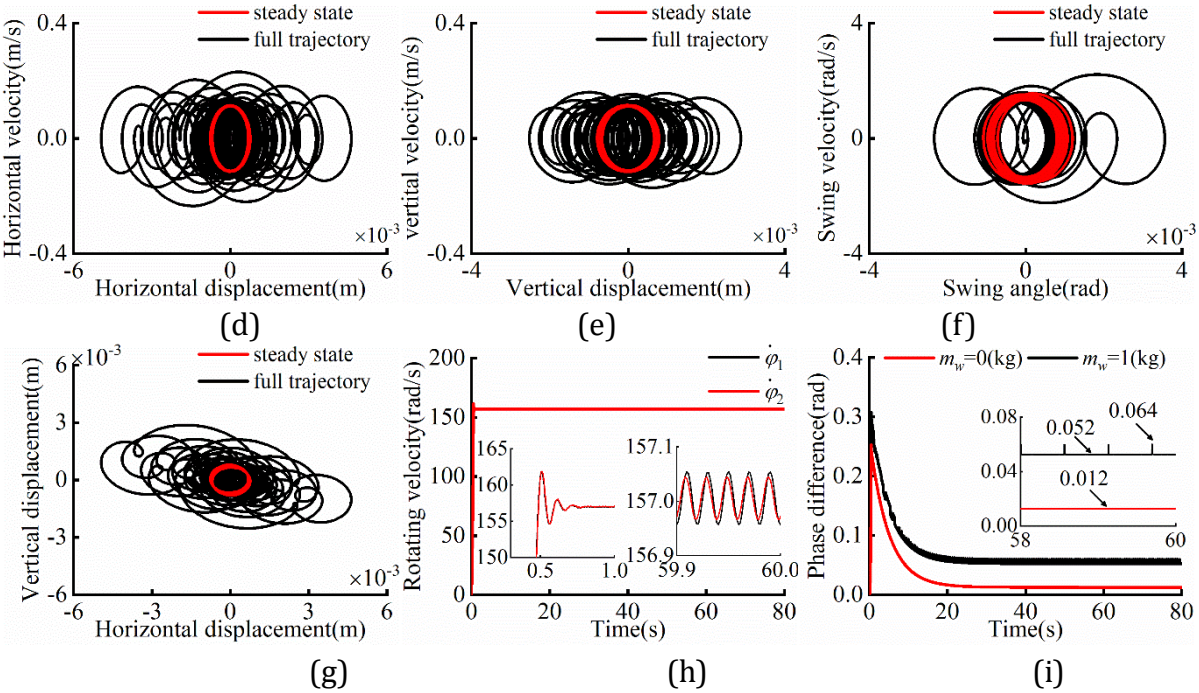

Fig. 2. Numerical simulation results of the system when m_w=1kg

Fig. 3 shows the dynamic characteristics of the vibration system under the impact of 4kg material. In the x and ψ directions, the displacement response fluctuates significantly, as shown in Fig. 3(a) and (c). In the y direction, the displacement response fluctuates more violently, with a maximum amplitude of 1.8mm, as shown in Fig. 3(b). In the x, y and ψ directions, the violent fluctuations of displacement and velocity lead to the serious deviation of the trajectory of the phase diagram, and the number of orbits increases significantly, indicating that the motion of the system in the x, y and ψ directions is in a chaotic state, as shown in Fig. 3(d), (e) and (f). On the whole, the vibration system is affected by the impact of materials, and the motion state of the system is unstable, without stable running track, as shown in Fig. 3(g). When the material mass is increased to 4kg, the stable speed of the two motors is still maintained at 157rad/s, as shown in Fig. 3(h). Compared with no material impact, the rotor phase difference of the two motors increased by 0.046rad, and the material collision with the screen caused the instantaneous phase of the motor to fluctuate within the range of 0.02rad to 0.06rad, and the rotor phase difference could not be restored to the stable value, as shown in Fig. 3(i). This shows that when the system sieving large mass materials, the stable motion of the vibrating body cannot be realized only by the system self-synchronous coupling.

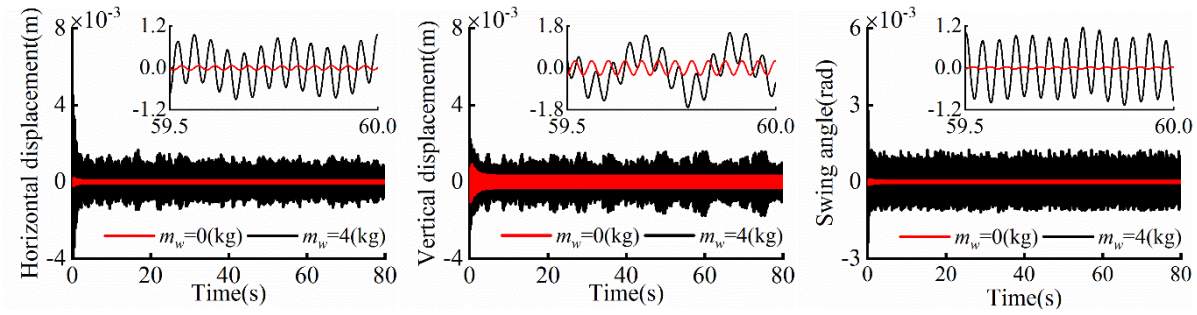

ISSN: 1813-4890

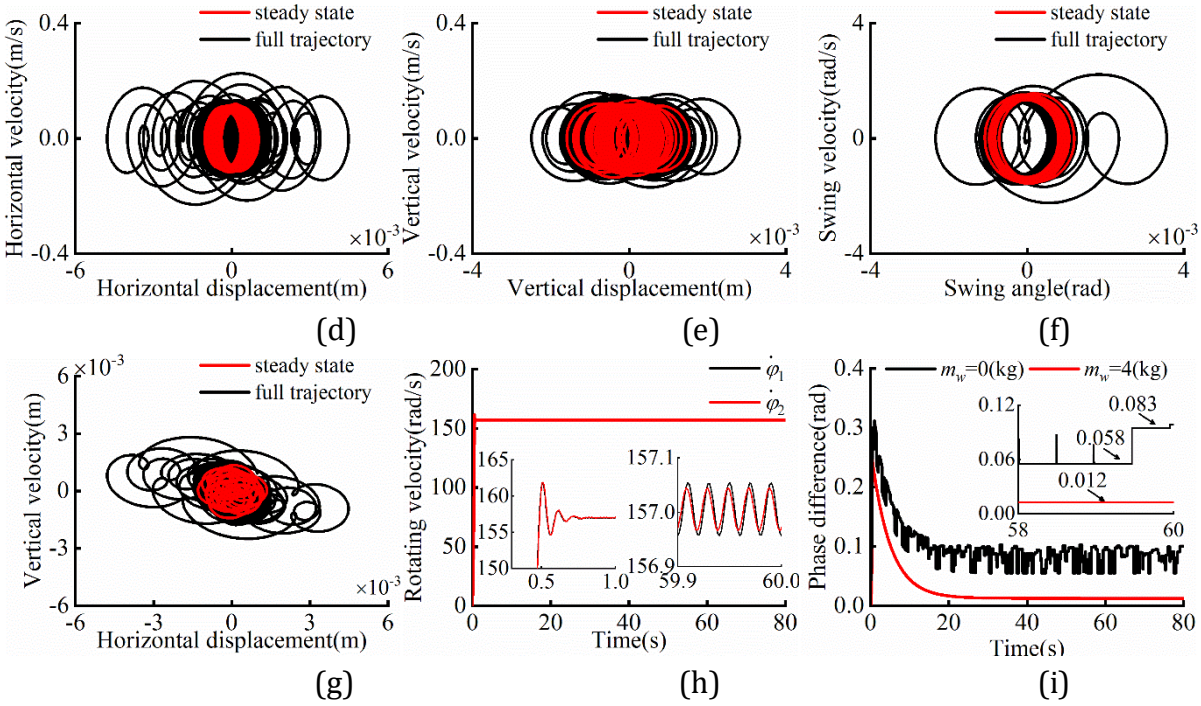

Fig. 3. Numerical simulation results of the system when m_w=4kg

3.2. The velocity bifurcation of the vibrating body

Assuming that the bifurcation coefficient is determined by the recovery coefficient R and the motor speed ω_m and material quality m_w. When R=0.1, ω_m=157rad/s, the velocity bifurcation diagram of the vibrating body under the impact of different mass materials is shown in Fig. 4. When the m_w is less than 2.4kg, the vibrating body exhibits stable double periodic motion in the x and y directions, the ψ direction is a single cycle motion. As the mass of the material increases, when the m_w is between 2.4% -6.9%, the motion of the vibrating body in all directions changes from double periodic motion to multi periodic motion. When the m_w exceeds 6.9kg, the motion of the vibrating body in all directions gradually evolves into chaotic motion. It can be seen that material impact has a significant impact on the motion stability of the vibrating body. As the mass ratio of the material to the vibrating body increases, the motion state of the vibrating body gradually tends towards chaos.

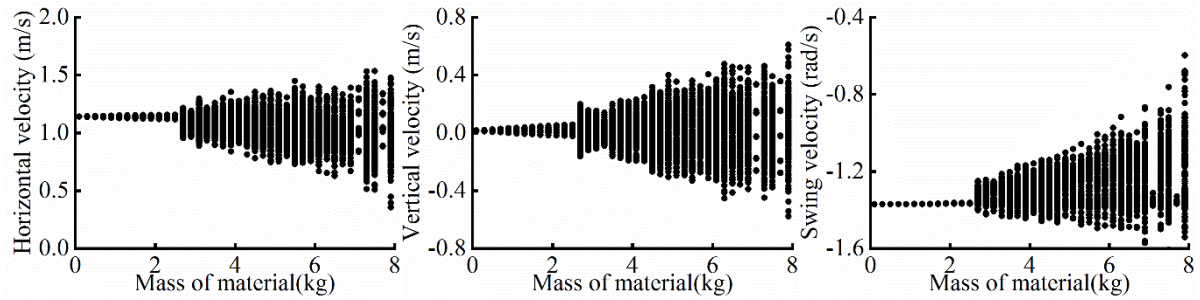

Fig. 4. Velocity bifurcation diagram of vibrating body

4. Conclusion

In this paper, the nonlinear dynamic characteristics of dual-rotor vibrating screen under material impact are analyzed. The main conclusions are as follows:

(1) The motion of vibrating body in horizontal and vertical direction is significantly affected by the impact of material, while the swinging direction is less affected. With the increase of the mass ratio between the material and the vibrating body, the motion path of the vibrating body

center gradually changes from ellipse to chaos. The motion state of the system is bifurcated from single-period motion to multi-period motion, and gradually evolves into chaotic motion. Similarly, the increase of the material mass leads to the abrupt increase of the phase difference of the two rotors, and the self-synchronization cannot be stably realized. Material impact has no effect on motor speed.

(2) The stability of periodic motion of a dual-rotor vibration system is studied, and the global bifurcation process from periodic motion to chaotic motion is explained. The parameter range of periodic motion is: single periodic motion when μ_m is less than 2.4%; multi-periodic motion when μ_m is between 2.4% and 6.9%; and chaotic motion when μ_m is greater than 6.9%. The bifurcation analysis of the system motion is helpful to judge the motion state of the vibration system in practical engineering.

Acknowledgements

This work was supported by Sichuan Science and Technology Program (2022YFQ0064) and Chengdu International Science and Technology Cooperation Projects (2021-GH02-00083-HZ)

References

[1] Z.R. Gao, A.R. Wei and X. Ma: Synchronization Characteristics Study on the Vibration Screen Actuated by Two Motors Considering Material Screening , China mining magazine. 31 (2022) No.S1, p.298-304. (In Chinese)

[2] X.X. Kong, J.X. Xing and B.C. Wen: Analysis of Motion of the Part on the Linear Vibratory Conveyor, Journal of Northeastern University (Natural Science). 36 (2015) No.6, p.827-831. (In Chinese)

[3] X.X. Kong, C.Z. Chen and B.C. Wen: Dynamic and Stability Analysis of the Vibratory Feeder and Parts Considering Interactions in the Hop and the Hop-sliding Regimes, Nonlinear Dynamics. 93 (2018) No.4, p.2213-2232. (In Chinese)

[4] Z.Q. Wang, L.P. Peng, C.L. Zhang, et al. Research on Impact Characteristics of Screening Coals on Vibrating Screen Based on Discrete-finite Element Method, Energy Sources Part a-recovery Utilization and Environmental Effects. 42 (2019) No.16, p.1963-1976.

[5] Z.Q. Wang, C.S. Liu, J.D. Wu, et al. Impact of Screening Coals on Screen Surface and Multi-index Optimization for Coal Cleaning Production, Journal of Cleaner Production. 187 (2018), p.562-575.

[6] Z.L. Huang, G.Q. Song, Z.C. Zhang, et al. Control Synchronization of two Nonidentical Homodromy Exciters in Nonlinear Coupled Vibration System, IEEE Access. (2019) No.7, p.109934-109944.

[7] Z.L. Huang, Y.M. Li, G.Q. Song, et al. Velocity and Phase Adjacent Cross-coupling Synchronous Control of Multi-exciters in Vibration System Considering Material Influence, IEEE Access. (2019) No.7, p.63204-63216.

[8] Y.J. Hou, G. Xiong, P. Fang, et al. Study on Stability of Self-synchronous Far-resonant Vibrating System of two Eccentric Rotors Considering Material Impact, Journal of Mechanical Science and Technology. 35 (2021) No.8, p.3271-3279.

[9] Y.J. Hou, G. Xiong, P. Fang, et al. Stability and Synchronous Characteristics of Dual-rotors Vibrating System Considering the Material Effects, Proceedings of The Institution of Mechanical Engineers Part K- Journal of Multi-body Dynamics. 236 (2022) No.1,p.15-30.